DYNAMIC ANALYSIS OF CYLINDRICAL SHELL PANELS. A MAEM SOLUTION

Aristophanes J. Yiotis and John T. Katsikadelis
School of Civil Engineering, National Technical University of Athens
e-mail: fgiotis@otenet.gr
e-mail: jkats@central.ntua.gr; web page: http://users.ntua.gr/jkats

Keywords: Meshless Analog Equation Method (MAEM), Dynamic Analysis, Radial Basis Functions (RBFs), partial differential equations, cylindrical shells.

Abstract. *The MAEM (Meshless Analog Equation Method), a purely mesh-free method, is applied to the dynamic analysis of cylindrical shell panels. The method is based on the principle of the analog equation, which converts the three governing partial differential equations in terms of displacements into three uncoupled substitute equations, two second order equations and one fourth order equation, under fictitious sources. The fictitious sources are represented by series of RBFs (Radial Basis Functions) of MQ (multiquadric) type and the substitute equations are integrated. This integration allows the representation of the sought solution by new RBFs, which approximate accurately not only the displacements but also their derivatives involved in the governing equations. Then, inserting the approximate solution in the original differential equations and the associated boundary and initial conditions and collocating at a predefined set of mesh-free nodal points, a system of ordinary differential equations results, the solution of which gives the unknown coefficients and then the displacements. The method is illustrated by analyzing several shell panels. The studied examples demonstrate the efficiency and the accuracy of the presented method.*

1 INTRODUCTION

The practical importance of thin shells in structural, mechanical and aerospace engineering applications has made vibration analysis essential in the planning process in order to achieve a better and more reliable design. Extensive research has been carried out by numerous researchers on this particular research topic.

For the dynamic analysis of linear elastic thin shells characterized by complex geometry, loading and boundary conditions, numerical methods, such as the FDM and especially the FEM have been used [1]. Both of these methods, in spite of some shortcomings, have been successfully employed for the solution of a variety of static and dynamic shell problems. The BEM has been proven an efficient alternative to the domain type methods, especially for thin elastic shallow shells [2], or combined with the AEM for cylindrical shells [3].

However, these methods require the design of meshes which is an extremely tedious and time-consuming process. In light of decreasing computer costs and increasing manpower costs, meshless methods (MM) present an attractive alternative to FEM or BEM, especial for shell structures that are very complex both in the field variable expression and the geometry representation. Another disadvantage of these methods is that their convergence rate is of second order [4].

Comprehensive descriptions of different MM are presented in [5-6] and in a review paper [7].

The mesh-free MQ-RBFs (multiquadric radial basis functions) method presented in [8] has attracted the interest of the investigators, because it enjoys exponential convergence and is very simple to implement. Recently using this method, papers dealing with the static analysis and vibration of composite shells [9] and the static analysis of cross-ply laminated shells [10] have appeared. The major drawback of this method is the ill-conditioning of the coefficient matrix. Besides, the inability to accurately approximate the derivatives of the sought solution renders the method inappropriate for a strong formulation of the problem. These drawbacks, inherent in the standard MQ-RBF method, are overcome by the new RBF method presented recently by Katsikadelis [11-15]. Another important issue is the implementation of multiple boundary conditions for equations of order higher than two. In this investigation the δ-technique is employed [16] for the fourth order equation. The problem of multiple boundary conditions does not appear when the shell is modeled as a three-dimensional body [17].

Following two papers presented recently for the static analysis [18] and buckling of cylindrical shells [19] ,the method is now extended to the dynamic problem of cylindrical shell panels as described in Section 3. In Section 2, the statement of the problem is presented, while several example problems are worked out in Section 4, which illustrate the applicability of the method and demonstrate its efficiency and accuracy. Finally, Section 5 includes certain conclusions drawn from this investigation.

2 STATEMENT OF THE PROBLEM

The Flügge type differential equations are used , which for thin-walled cylindrical shells of uniform thickness h , (Fig. 1) made of an isotropic, linearly elastic material are written as [20-21]:

$$u_{,xx}+\frac{1-\nu}{2}u_{,ss}+\frac{1+\nu}{2}v_{,xs}+\frac{\nu}{R}w_{,x}-\frac{h^2}{12}\frac{1}{R}[w_{,xxx} -\frac{1-\nu}{2}R(\frac{w_{,xs}}{R}+\frac{u_{,s}}{R^2})_{,s}]-c_1\dot{u}=-\frac{1-\nu^2}{Eh}(q_x-\rho h\ddot{u}) \tag{1a}$$

$$v_{,ss}+\frac{1-\nu}{2}v_{,xx}+\frac{1+\nu}{2}u_{,xs}+(\frac{w}{R})_{,s}+\frac{h^2}{12}\frac{1}{R^2}[\frac{3(1-\nu)}{2}v_{,xx} -\frac{(3-\nu)}{2}Rw_{,xxs}-R_{,s}(w_{,ss}+\frac{w}{R^2}+\frac{R_{,s}}{R^2}v)]-c_1\dot{v}=-\frac{1-\nu^2}{Eh}(q_s-\rho h\ddot{v}) \tag{1b}$$

$$\nabla^4 w+\frac{w_{,ss}}{R^2}+(\frac{w}{R^2})_{,ss}+\frac{w}{R^4}-\frac{1}{R}u_{,xxx}+\frac{1-\nu}{2}(\frac{u_{,xs}}{R})_{,s}-\frac{3-\nu}{2}(\frac{v}{R})_{,xxs} +(\frac{R_{,s}}{R^2}v)_{,ss}+\frac{R_{,s}}{R^4}v+\frac{12}{h^2}\frac{1}{R}(v_{,s}+\frac{w}{R}+\nu u_{,x})+c_1\dot{w}=-\frac{12(1-\nu^2)}{Eh^3}(-q_z+\rho h\ddot{w}) \tag{1c}$$

where $\nabla^4=\frac{\partial^4}{\partial x^4}+\frac{2\partial^4}{\partial x^2\partial s^2}+\frac{\partial^4}{\partial s^4}$ is the biharmonic operator. The parametric lines x $(s=const.)$ and s $(x=const.)$ are assumed to be lines of curvature: x measured along the length axis of the shell and s is the length of the curve $x=const.$, while z is measured along the normal to the middle surface of the shell (Fig. 1). Since a cylindrical surface can be mapped isometrically on a plane, the orthogonal curvilinear coordinates x and s may be viewed as orthogonal plane coordinates. The functions $u(x,s)$ $v(x,s)$ and $w(x,s)$ represent the axial, circumferential and normal displacements; $R=R(s)$ is the variable radius of curvature of the cross-section of the shell, h its thickness, ρ the mass density per unit volume of the material of the shell and c_1 its damping.

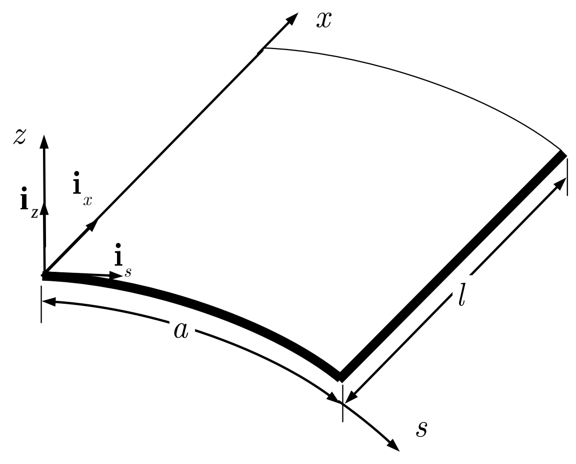

Figure 1: Cylindrical shell.

Moreover, Eqs (1) must satisfy the following boundary conditions [21]:

On a curved edge ($x=0$ or $x=l$)

$$u=\bar{u} \text{ or } N_x=\bar{N}_x \tag{2a}$$

$$v=\bar{v} \text{ or } T_{xs}=\bar{T}_{xs} \tag{2b}$$

$$w=\bar{w} \text{ or } V_x=\bar{V}_x \tag{2c}$$

$$\theta_x=\bar{\theta}_x \text{ or } M_x=\bar{M}_x\ , \quad (\theta_x=-\frac{\partial w}{\partial x}) \tag{2d}$$

On a straight edge ($s=0$ *or* $s=a$ *)*

$$u=\bar{u} \text{ or } T_{sx}=\bar{T}_{sx} \tag{2e}$$

$$v=\bar{v} \text{ or } N_s=\bar{N}_s \tag{2f}$$

$$w=\bar{w} \text{ or } V_s=\bar{V}_s \tag{2g}$$

$$\theta_s=\bar{\theta}_s \text{ or } M_s=\bar{M}_s, \quad (\theta_s=\frac{v}{R}-\frac{\partial w}{\partial s}) \tag{2h}$$

the over bar designates a prescribed quantity. Moreover, the following corner conditions must be satisfied [22]

$$w=\bar{w} \text{ or } (M_{xs}-M_{sx})_k=\bar{F}_k, \quad k=1,2,3,4 \tag{2i}$$

Furthermore the initial conditions are:

$$w(\mathbf{x},0)=g_3(\mathbf{x}), \qquad \dot{w}(\mathbf{x},0)=h_3(\mathbf{x}) \tag{3a}$$

$$u(\mathbf{x},0)=g_1(\mathbf{x}), \qquad \dot{u}(\mathbf{x},0)=h_1(\mathbf{x}) \tag{3b}$$

$$v(\mathbf{x},0)=g_2(\mathbf{x}), \qquad \dot{v}(\mathbf{x},0)=h_2(\mathbf{x}) \tag{3c}$$

where $g_i(\mathbf{x})$, $h_i(\mathbf{x})$, $\mathbf{x}=(x,s)$ $(i=1,2,3)$ are specified functions.

The stress resultants N_x, N_s, N_{xs}, N_{sx}, M_x, M_s, M_{xs}, M_{sx}, Q_x, Q_s, the effective tangential membrane and transverse shear forces at the edges $x=0,l$ T_{xs} and V_x and the effective tangential membrane and transverse shear force at edges $s=0,a$ T_{sx} and V_s are expressed in terms of the displacements as in [18].

3 THE MAEM SOLUTION

Let u,v and w be the sought solution. Since Eqs (1) are of the second order with respect to u,v and of the fourth order with respect to w, the analog equations that are convenient to use are [23]

$$\nabla^2 u=b_1(\mathbf{x},t) \qquad \nabla^2 v=b_2(\mathbf{x},t) \qquad \nabla^4 w=b_3(\mathbf{x},t) \tag{4a,b,c}$$

where $b_i=b_i(\mathbf{x},t)$ $(i=1,2,3)$ are unknown fictitious sources. These fictitious sources depend on time, which is regarded as a parameter. They can be established as follows.

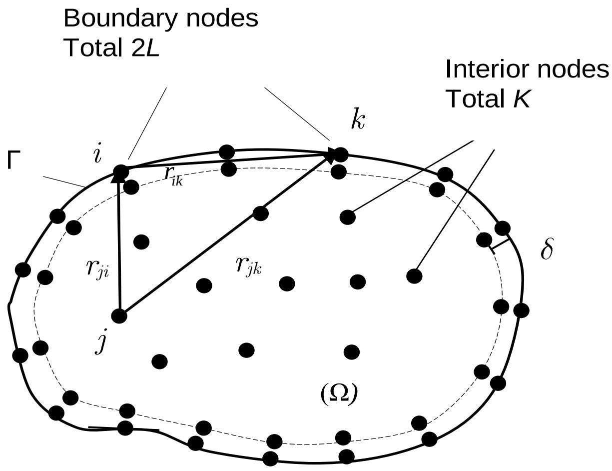

Figure 2: Boundary and domain nodal points.

Approximating the fictitious sources with MQ-RBFs series, we can write

$$\nabla^2 u \simeq \sum_{j=1}^{K+L} a_j^{(1)}(t) f_j \qquad \nabla^2 v \simeq \sum_{j=1}^{K+L} a_j^{(2)}(t) f_j \qquad \nabla^4 w \simeq \sum_{j=1}^{K+2L} a_j^{(3)}(t) f_j \tag{5a,b,c}$$

where $f_j = \sqrt{r^2 + c^2}$, $r = |\mathbf{x} - \mathbf{x}_j|$, c the shape parameter with K, L representing the number of collocating points inside Ω and on Γ, respectively (see Fig. 2) and $a_j^{(1)}$, $a_j^{(2)}$, $a_j^{(3)}$ time dependent coefficients to be determined. Note that the derivatives of the membrane displacements u, v are collocated in K domain and L boundary points, while the derivatives of the normal displacement w according to the δ-technique [24] are collocated in K domain and $2L$ boundary points.

Equations (5) can be directly integrated to yield

$$u \simeq \sum_{j=1}^{K+L} a_j^{(1)}(t) \hat{u}_j \qquad v \simeq \sum_{j=1}^{K+L} a_j^{(2)}(t) \hat{v}_j \qquad w \simeq \sum_{j=1}^{K+2L} a_j^{(3)}(t) \hat{w}_j \tag{6a,b,c}$$

where $\hat{u}_j(r), \hat{v}_j(r), \hat{w}_j(r)$ are solutions of the equations

$$\nabla^2 \hat{u} = f_j(r) \qquad \nabla^2 \hat{v} = f_j(r) \qquad \nabla^4 \hat{w} = f_j(r) \tag{7a,b,c}$$

The solution of Eqs (7) can be readily obtained after writing them in polar coordinates. Thus for the second order equations we have

$$\nabla^2 \hat{u} = \frac{1}{r}\frac{d}{dr}\left(r \frac{d\hat{u}_j}{dr} \right) = f_j(r) \tag{8}$$

which after integration gives

$$\hat{u}_j = \frac{1}{9} f_j^3 + \frac{1}{3} f_j c^2 - \frac{c^3}{3} \ln\ c + f_j\ \ + G_1 \ln(r) + H_1 \tag{9}$$

Similarly, we have

$$\hat{v}_j = \frac{1}{9} f_j^3 + \frac{1}{3} f_j c^2 - \frac{c^3}{3} \ln\ c + f_j\ \ + G_2 \ln(r) + H_2 \tag{10}$$

The regularity condition at $r = 0$ demands $G_1 = G_2 = 0$. The remaining constants H_1, H_2 together with the shape parameter c, if not arbitrarily specified, can be determined through an optimization procedure, such that to ensure regularity of coefficients matrix (control of the condition number) and minimization of the error. Since it has been shown that the coefficient matrix resulting from the new RBFs is always invertible [25], we take in this analysis for convenience $H_1 = H_2 = 0$. Thus only the shape parameter c is involved in the error minimization precedure [11].

For the fourth order equation, we can write

$$\nabla^4 \hat{w} = \nabla^2(\nabla^2 \hat{w}) = f_j \tag{11}$$

which yields after integration and removal of the singular terms as well as the terms including the arbitrary constants [26]

$$\hat{w}_j = -\frac{7}{60} c^4 f_j + \frac{2}{45} c^2 f_j^3 + \frac{1}{225} f_j^5 + \frac{2c^2 - 5r^2}{60} c^3 \ln(c + f_j) + \frac{1}{12} r^2 c^3 \tag{12}$$

The spacial and time derivatives of the displacements are obtained by direct differentiation of Eqs. (6):

$$u_{,ikl} \simeq \sum_{j=1}^{K+L} a_j^{(1)} \hat{u}_{j,ikl} \qquad v_{,ikl} \simeq \sum_{j=1}^{K+L} a_j^{(2)} \hat{v}_{j,ikl} \qquad w_{,ikl} \simeq \sum_{j=1}^{K+2L} a_j^{(3)} \hat{w}_{j,ikl} \tag{13a,b,c}$$

$$\dot{u} \simeq \sum_{j=1}^{K+L} \dot{a}_j^{(1)}(t) \hat{u}_j \qquad \dot{v} \simeq \sum_{j=1}^{K+L} \dot{a}_j^{(2)}(t) \hat{v}_j \qquad \dot{w} \simeq \sum_{j=1}^{K+2L} \dot{a}_j^{(3)}(t) \hat{w}_j \tag{14a,b,c}$$

$$\ddot{u} \simeq \sum_{j=1}^{K+L} \ddot{a}_j^{(1)}(t)\hat{u}_j \qquad \ddot{v} \simeq \sum_{j=1}^{K+L} \ddot{a}_j^{(2)}(t)\hat{v}_j \qquad \ddot{w} \simeq \sum_{j=1}^{K+2L} \ddot{a}_j^{(3)}(t)\hat{w}_j \tag{15a,b,c}$$

where i,k,l stand for x,s.

Collocating Eqs. (1) at the K nodal points inside Ω and the four boundary conditions, Eqs. (2), at the L boundary nodal points (Fig. 2) and inserting Eqs. (6-13-15) in the resulting expressions using the well known δ-technique [24] a system of ordinary differential equations of motion is obtained, namely

$$\mathbf{M}\ddot{\mathbf{a}} + \mathbf{C}_1\dot{\mathbf{a}} + \mathbf{K}\mathbf{a} = \mathbf{g} \tag{16}$$

where $\mathbf{M}$, $\mathbf{C}_1$ and $\mathbf{K}$ are known square matrices having dimension; $3K+4L$; $\mathbf{g}$ is a vector including the $3K$ values of the external load $g(\mathbf{x},t)$ and $\mathbf{a}$ is the vector of the $3K+4L$ values of the unknown time dependent coefficients $a_j^{(1)}(t)$, $a_j^{(2)}(t)$, $a_j^{(3)}(t)$.

Eq. (16) is the semi-discretized equation of motion of the cylindrical shell with $\mathbf{M}$, $\mathbf{C}_1$ and $\mathbf{K}$ representing generalized mass, damping and stiffness matrices, respectively. It can be solved numerically, using any time step integration technique to establish the time dependent unknown coefficients, e.g. [27-28]. The initial conditions of Eq. (16) are obtained from Eqs. (6) and (14) on the basis of Eqs. (3) as follows:

$$\mathbf{a}_\mathbf{j}^{(1)}(\mathbf{0}) = \hat{\mathbf{u}}_\mathbf{j}{}^{-1}\mathbf{g}_1(\mathbf{x}) \qquad \dot{\mathbf{a}}_\mathbf{j}^{(1)}(\mathbf{0}) = \hat{\mathbf{u}}_\mathbf{j}{}^{-1}\mathbf{h}_1(\mathbf{x}) \tag{17a}$$

$$\mathbf{a}_\mathbf{j}^{(2)}(\mathbf{0}) = \hat{\mathbf{v}}_\mathbf{j}{}^{-1}\mathbf{g}_2(\mathbf{x}) \qquad \dot{\mathbf{a}}_\mathbf{j}^{(2)}(\mathbf{0}) = \hat{\mathbf{v}}_\mathbf{j}{}^{-1}\mathbf{h}_2(\mathbf{x}) \tag{17b}$$

$$\mathbf{a}_\mathbf{j}^{(3)}(\mathbf{0}) = \hat{\mathbf{w}}_\mathbf{j}{}^{-1}\mathbf{g}_3(\mathbf{x}) \qquad \dot{\mathbf{a}}_\mathbf{j}^{(3)}(\mathbf{0}) = \hat{\mathbf{w}}_\mathbf{j}{}^{-1}\mathbf{h}_3(\mathbf{x}) \tag{17c}$$

Once the coefficients $a_j^{(1)}$, $a_j^{(2)}$, $a_j^{(3)}$ have been computed, the field functions *u, v,* w and their derivatives can be evaluated using relations (6) and (13-15) respectively. The stress resultants can be found readily [18].

3.1 Free vibrations of cylindrical shells

In this case $\mathbf{g}(t)=0$, $\mathbf{C}_1 = 0$, the equation of motion (16) takes the form

$$\mathbf{M}\ddot{\mathbf{a}} + \mathbf{K}\mathbf{a} = 0 \tag{18}$$

and the boundary conditions (2) become homogeneous. By setting

$$\mathbf{a(t)} = \mathbf{a}e^{-i\omega t} \tag{19}$$

Eq. (18) becomes

$$\left[\mathbf{K} - \omega^2\mathbf{M}\right]\mathbf{a} = \mathbf{0} \tag{20}$$

which gives the eigenfrequencies ω_i and the eigenvectors $\mathbf{a}_\mathbf{i}$ $i = 1,2,\ldots,3K+4L$. Subsequently, using $\mathbf{a} = \mathbf{a}_\mathbf{i}$ in Eqs. (6) we obtain the mode shapes.

The accuracy of the approximation (6) depends heavily on c. This was also verified in this case. Thus we come across to the problem of choosing a good value for c. Several methods for selecting a good value for c in two dimensional problems have been suggested [18]. For the problem at hand the optimal value of c is obtained by the search method, namely the value of c which gives the minimum value of the eigenfrequency ω. It was observed that the optimum c that gives the minimum first eigenvalue differs negligibly from that yielding the minimum higher eigenvalues. Therefore the same optimum value of c can be used to avoid the search method for higher eigenvalues.

4 NUMERICAL EXAMPLES

On the basis of the above analysis a Fortran program has been written. The expressions of the derivatives involved in Eqs (1)-(2) have been obtained using the symbolic language MAPLE. The efficiency and accuracy of the developed method is demonstrated by studying the eigenfrequencies of circular cylindrical panels of Fig. 3 under different sets of boundary conditions. The NASTRAN FEM code with 400 rectangular elements has been used to compare the results.

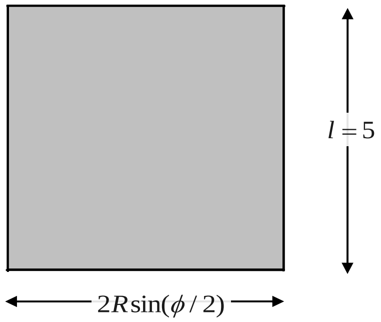

a. planform

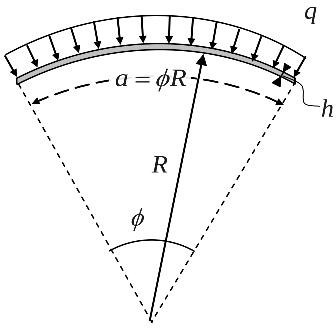

b. cross-section

Figure 3: Geometry of the circular cylindrical shell.

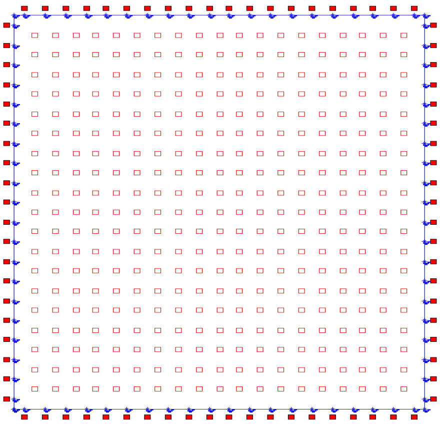

(a) MAEM

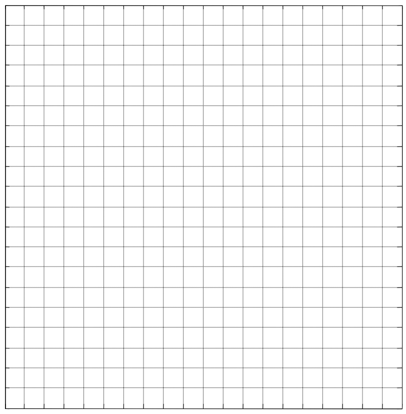

(b) FEM

Figure 4: Shell discretization.

4.1 Example 1

The non-dimensional eigenfrequency parameter $\Omega_f = R\omega\sqrt{(1-\nu^2)\rho/E}$ of a simply supported circular cylindrical shell panel with movable curved edges in the axial direction ($N_x = v = w = M_x = 0$ along the curved edges and $u = v = w = M_s = 0$ along the straight edges) has been studied. The first six eigenfrequency parameters are given in Table 1 as compared with a FEM solution. The first vibration mode for the normal displacement is shown in Fig. 5. The numerical results have been obtained with $L = 80$, $K = 361$ and $\delta = 1.e-4$. The optimal value is $c_{opt} = 0.06$ for the first mode, which has also been used for the next five modes. The employed data are: $E = 21\times10^6\,\mathrm{kN/m^2}$, $h = 0.10m$, $R = 10.00\,m$, $l = 5.00\,m$, $a = 5.00\mathrm{m}$, $\nu = 0.30$.

Table 1: Eigenfrequency parameters of the shell in Example 1.

mode	c	$\Omega_f = R\omega\sqrt{(1-\nu^2)\rho/E}$	
		MAEM	FEM
1	0.06	0.7035	0.692
2	0.06	0.8705	0.865
3	0.06	1.0469	1.043
4	0.06	1.1128	1.109
5	0.06	1.1875	1.201
6	0.06	1.4020	1.493

4.2 Example 2

In this example a clamped ($u = v = w = \theta_x = 0$ along the curved edges and $u = v = w = \theta_s = 0$ along the straight edges) cylindrical shell panel is analyzed. The numerical results have been obtained with $L = 80$, $K = 361$ and $\delta = 1.e-4$. The other employed data are: $E = 21\times10^6\,\mathrm{kN/m^2}$, $R = 9.896\,m$, $l = 4.948\,m$, $a = 5.00m$, $\phi = 28.93°$, $\nu = 0.30$. Two cases have been studied: (a) $2R\sin(\phi/2)/h = 100$ and (b) $2R\sin(\phi/2)/h = 20$. The first eight eigenfrequency parameters are shown in Tables 2 and 3 as compared with an analytical solution [29]. The first and second vibration modes for the normal displacement for (a) case are shown in Fig. 6 and 7. The optimal value is $c_{opt} = 0.05$, which has been used for all the computed modes.

.

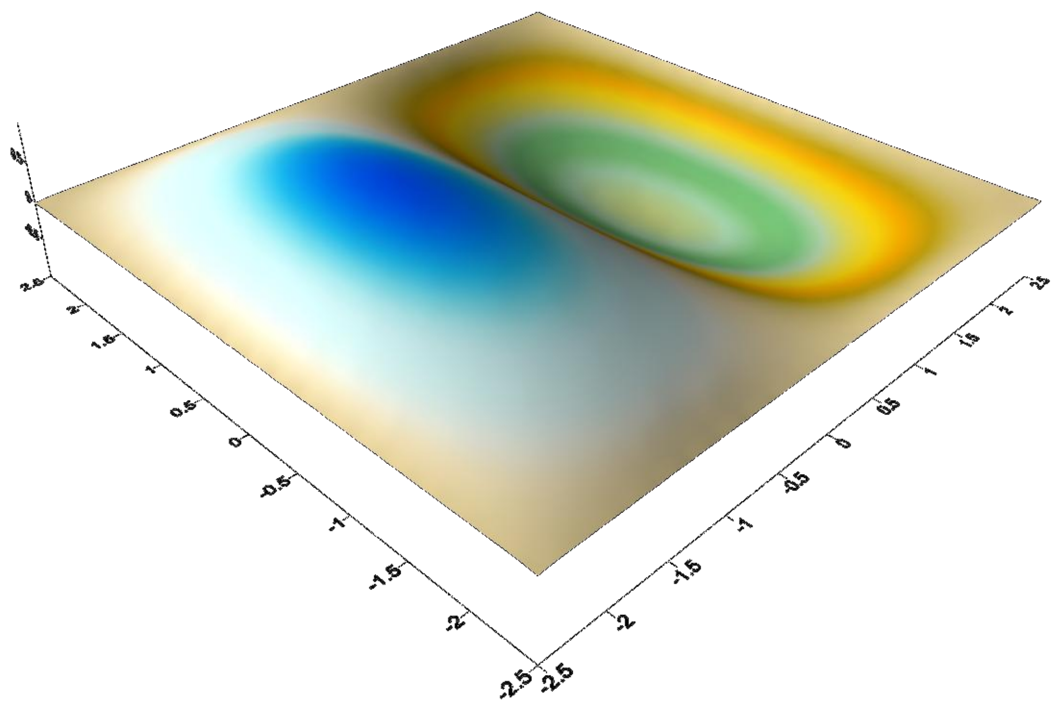

Figure 5: 1st vibration mode of the shell in Example 1.

5 CONCLUSIONS

The MAEM, a truly meshless method, has been applied for the dynamic analysis of thin cylindrical shell panels. The method is based on the principle of the analog equation, which converts the original equations into three substitute equations. The use of MQ-RBFs to approximate the fictitious sources allows, after direct integration, the approximation of the sought solutions by new RBFs, which approximate accurately not only the solution but also its derivatives. Thus the strong formulation of the problem avoids the drawbacks inherent in the conventional MQ-RBFs, while it maintains all the advantages of the truly mess-free methods. A method is presented to obtain optimum values for the shape parameter, which eliminates the uncertainty of its choice. It was observed that the optimum value of the shape parameter for the first mode can be used to obtain also the eigenfrequencies corresponding to higher modes. The solution algorithm is simple to construct and reasonably easy to program. The presented examples demonstrate the efficiency and accuracy of the method and show that the MAEM provides an efficient solver of difficult problems in engineering analysis.

Table 2: Eigenfrequency parameters of the shell in Example 2: case a .

mode	c	$\Omega_f = \dfrac{2l\omega R\sin(\phi/2)}{h}\sqrt{12\times(1-\nu^2)\rho/E}$	
		MAEM	[29]
1	0.05	101.568	99.263
2	0.05	120.150	119.00
3	0.05	152.806	151.13
4	0.05	157.323	156.35
5	0.05	173.581	172.52
6	0.05	191.739	192.43
7	0.05	201.702	201.67
8	0.05	206.381	207.80

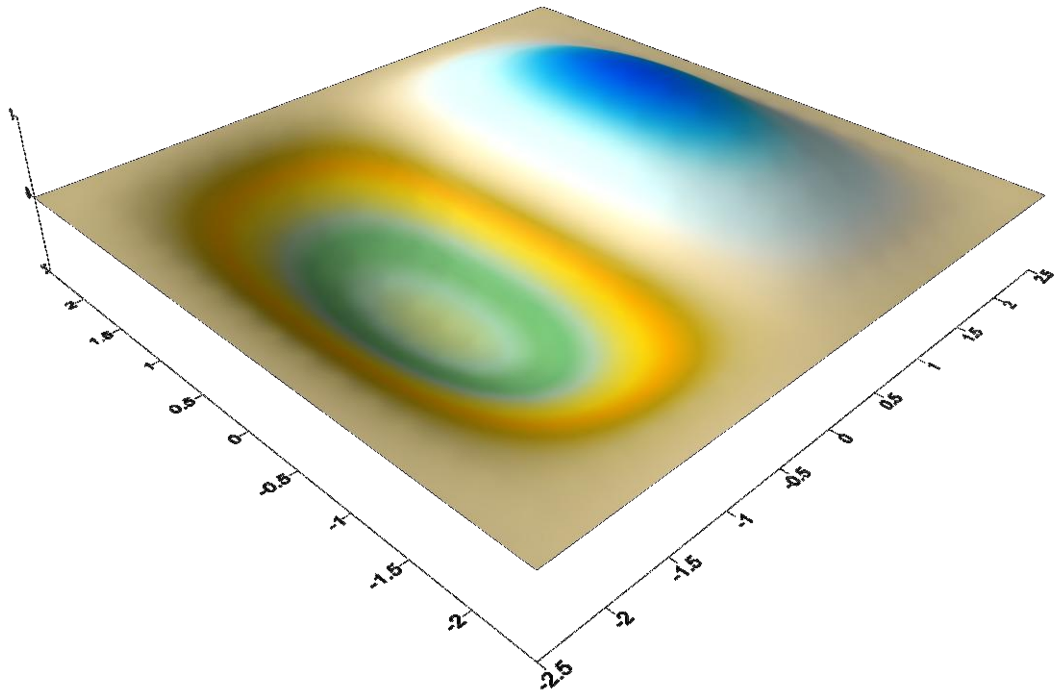

Figure 6: 1st vibration mode of the shell in Example 2 : case (a).

Table 3: Eigenfrequency parameters of the shell in Example 2: case (b).

mode	c	$\Omega_f = \frac{2l\omega R\sin(\phi/2)}{h}\sqrt{12\times(1-\nu^2)\rho/E}$	
		MAEM	[29]
1	0.05	46.221	46.241
2	0.05	72.619	74.300
3	0.05	78.609	79.239
4	0.05	107.131	110.14
5	0.05	127.122	132.35
6	0.05	132.441	135.51
7	0.05	157.624	165.57
8	0.05	160.162	166.82

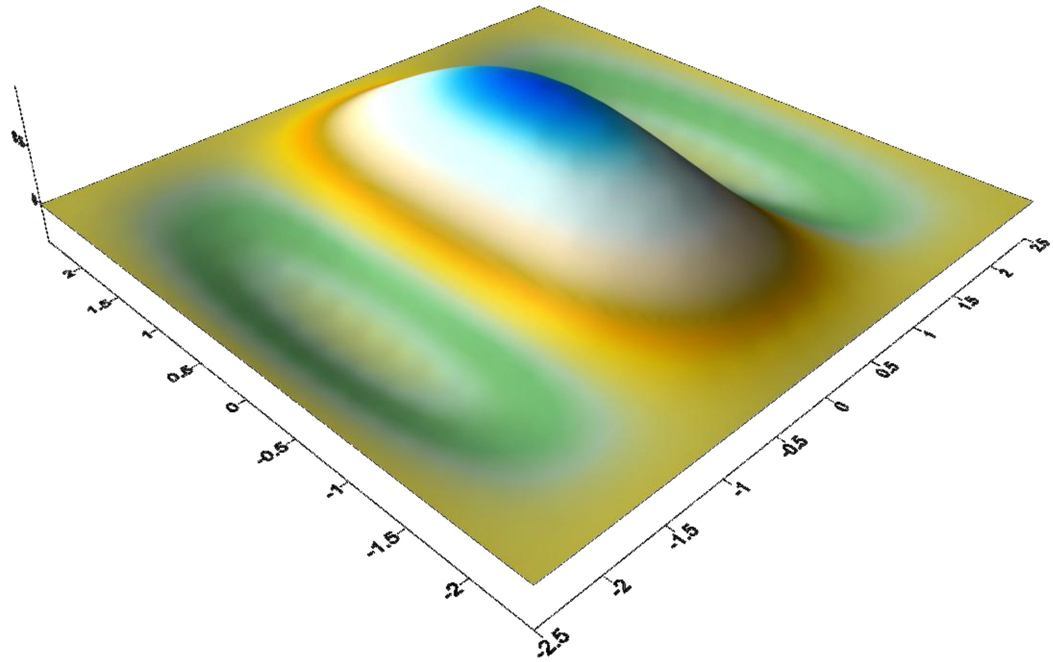

Figure 7: 2nd vibration mode of the shell in Example 2: case (a).

REFERENCES

[1] Lee S.J and Han S.E. (2001), "Free-vibration analysis of plates and shells with a nine-node assumed natural degenerated shell element", *Journal of Sound and Vibration*, Vol. 241(4), pp. 605-633.

[2] Beskos D. E. (1991), "Static and Dynamic Analysis of Shells, in: Boundary Element Analysis of Plates and Shells" (Ed. Beskos, D.E,), pp. 93-140, Springer-Verlag, Berlin.

[3] Yiotis A. J. and Katsikadelis J. T. (2000), "Static and Dynamic Analysis of Shell Panels Using the Analog Equation Method", *Computer Modeling in Engineering Science*, Vol. 1, No 2, pp. 95-103.

[4] Cheng A. H. D, Golbeg M. A., Kansa E. J. and Zammito G. (2003), "Exponential convergence and *h-c* multiquadric collocation method for partial differential equations", *Numerical Methods for Partial Differential Equations*, Vol. 19(5), pp. 571-594.

[5] Liu G. R. (2002), *Meshfree Methods: Moving Beyond the Finite Element Method*, CRC Press, New York.

[6] Liu G. R., Gu Y.T. (2005), *An Introduction to Meshfree Methods and Their Programming*. Springer, Dordrecht.

[7] Nguyen V.P., Rabczuk T., Bordas S. and Duflot M. (2008), "Meshless methods: a review and conputer implementation aspects", *Mathematics and Computers in Simulation*, Vol. 79, pp. 763-813.

[8] Kansa E.J. (2005), "Highly accurate methods for solving elliptic partial differential equations". In: Brebbia, C.A., Divo, E. and Poljak, D. (eds.), *Boundary Elements XXVII*, WIT Press, Southampton, pp. 5-15.

[9] Ferreira A.J.M., Roque C.M.C. and Jorge R.M.M., (2006), "Static and free vibration analysis of composite shells by radial basis functions", *Engineering Analysis with Boundary Elements*, Vol. 30, pp. 719-733.

[10] Ferreira A.J.M., Roque C.M.C. and Jorge R.M.M., (2006), "Modelling cross-ply laminated elastic shells by a higher-order theory and multiquadrics", *Computers and Structures*, Vol. 84, pp. 1288-1299.

[11] Katsikadelis J.T. (2006), "The meshless analog equation method. A new highly accurate truly mesh-free method for solving partial differential equations". In: Brebbia C.A. and Katsikadelis J.T., (eds), *Boundary Elements and other mesh reduction methods XXVIII*, WIT Press, Southampton, pp. 13-22.

[12] Katsikadelis J. T. (2008), "The 2D elastostatic problem in inhomogeneous anisotropic bodies by the meshless analog equation method MAEM", *Engineering Analysis with Boundary Elements*, Vol. 32, pp. 997-1005, (doi: 10.1016/ j.enganabound.2007.10.016).

[13] Katsikadelis J.T**.** (2008), "A generalized Ritz Method for Partial DifferentialEquations in Domains of Arbitrary Geometry Using Global Shape Functions", *Engineering Analysis with Boundary Elements*, Vol. 32 (5), pp. 353–367 (doi:10.1016/j. enganabound. 2007.001).

[14] Yiotis A. J and Katsikadelis J. T. (2008), "The Meshless Analog Equation Method for the solution of plate problems", *Proceedings of the 6th GRACM International Congress on Computational Mechanics*, Thessaloniki, Greece.

[15] Katsikadelis J. T. (2009), "The meshless analog equation method: I. Solution of elliptic partial differential equations", *Archive of Applied Mechanics*, Vol. 79, pp. 557-578.

[16] Jang S.K., Bert C.W. and Striz, A.G. (1989), "Application of differential quadrature to static analysis of structural components", *International Journal for Numerical Methods in Engineering*, Vol. 28, 3, pp. 561-577.

[17] Katsikadelis J. T. and Platanidi J. G. (2007), "3D Analysis of Thick Shells by the Meshless Analog Equation Method", *Proceedings of the 1st International Congress of Serbian Society of Mechanics*, pp. 475-484.

[18] Yiotis A. J. and Katsikadelis J. T., (2013), "Analysis of Cylindrical Shell Panels. A Meshless Solution", *Engineering Analysis with Boundary Elements*, Vol. 37, pp. 928-935.

[19] Yiotis A. J. and Katsikadelis J. T., (2013), "Buckling Analysis of Cylindrical Shell Panels. A Meshless Solution", *Archive of Applied Mechanics*, doi: 10.1007/s00419-014-0944-9.

[20] Flügge W. (1962), *Stresses in Shells*, Springer-Verlag, Berlin.

[21] Kraus H. (1967), *Thin elastic shells. An Introduction to the Theoretical Foundations and the Analysis of Their Static and Dynamic Behabior*, John Wiley and Sons, New York-London-Sydney.

[22] Leissa A.W. (1973), *Vibrations of Shells*, Scientific and Technical Information Office, NASA, Washington.

[23] Katsikadelis J. T. (2002), "The analog equation method. A boundary-only integral equation method for nonlinear static and dynamic problems in general bodies", *International Journal of Theoretical and Applied Mechanics, Archive of Applied Mechanics*, Vol. 27, pp. 13-38.

[24] Ferreira A.J.M., Roque C.M.C. and Martins P.A.L.S. (2005), "Analysis of thin isotropic rectangular and circular plates with multiquadrics", *Strength of Materials*, Vol. 37, 2, pp. 163-173.

[25] Sarra (2006), "Integrated Multiquadric Radial Basis Function Methods", *Computers and Mathematics with Applications*, Vol. 51 , pp. 1283-1296.

[26] Yao G., Tsai C.H. and Chen W. (2010), "The comparison of three meshless methods using radial basis functions for solving fourth-order partial differential equations", *Engineering Analysis with Boundary Elements*, Vol. 34, pp. 625-631.

[27] Katsikadelis J. T. (2014), *Boundary Element Method for Plate Analysis*, Academic Press, Elsevier, Amsterdam.

[28] Katsikadelis, J.T. (2014), "A New Direct Time Integration Method for the Equations of Motion in Structural Dynamics", *ZAMM*, *Zeitschrift für Angewandte Mathematik und Mechanik*, Vol. 94(9), pp. 757–774.

[29] Lim C.W. and Liew K. M. (1994), "A pb-2 Ritz formulation for flexural vibration of shallow cylindrical shells of rectangular planform", *Journal of Sound and Vibration*, Vol. 173(3), pp. 343-375.